

variation of D_{Mn} , with temperature, given as

$$D_{Mn} = 3.23 \exp\left(\frac{-36640}{T}\right)$$

is shown in Fig. 4. The derived activation energy for the diffusion of Mn in Pt, 305 kJ/mol, is close to the value of 286 kJ/mol reported by Kidson and Ross⁵ as the activation energy for the self-diffusion of Pt.

The agreement between the experimental data and Eq. [1] indicates that the rate of pick-up of Mn by the Pt foils is controlled by diffusion of Mn in Pt, and permits evaluation of the chemical diffusivity of Mn in Pt.

Grateful acknowledgement is made to the National Science Foundation who supported this work under their Grant Number DMR77-03426.

1. B. K. D. P. Rao and D. R. Gaskell: *Met. Trans. A*, 1981, vol. 12A, p. 207.
2. B. K. D. P. Rao and D. R. Gaskell: *Met. Trans. B*, in press.
3. B. K. D. P. Rao and D. R. Gaskell: *Met. Trans. B*, in press.
4. J. Crank: *The Mathematics of Diffusion*, p. 47, Oxford Press, London, 1956.
5. G. V. Kidson and R. Ross: *Proc. Int. Conf. Radiosotopes Sci. Res.*, Paris, 1957, vol. 1, p. 185.

The Effect of Temperature Dependent Electrical Conductivity on Flow and Temperature Fields in Slags in ESR Systems

M. CHOUDHARY AND J. SZEKELY

There are numerous metals processing operations, where a high current is passed through a molten, conducting medium and the resultant combined effect of "joule heating" and electromagnetic forces gives rise to convective flows. Electroslag refining, electroslag welding, aluminum smelting and the operation of various "submerged arc" furnaces are representative examples.

The recent mathematical models of these operations, relied on the simultaneous solution of Maxwell's equations, the Navier-Stokes equations and the thermal energy balance equation.¹⁻⁵

Two important assumption have been made, namely:

1) that fluid flow does not play a role in modifying the transport of current and

M. CHOUDHARY and J. SZEKELY are Research Associate and Professor, respectively, Department of Materials Science and Engineering, Massachusetts Institute of Technology, Cambridge, MA 02139.

Manuscript submitted December 4, 1980.

2) that the electrical conductivity of these systems is independent of temperature.

The former assumption is thought to be reasonable, because of the low value of the magnetic Reynolds number, however the second assumption is more questionable, because of the substantial temperature differences that may exist in these systems.

In a previous paper⁵ we have presented a somewhat *ad hoc* examination of the possible role played by a temperature dependent electrical conductivity in modifying the temperature fields in a laboratory scale ESR system. The purpose of this communication is to examine this problem in a more systematic manner.

The general mathematical description of the electromagnetic force field, temperature field and velocity field in ESR systems is available in previous publications;^{2,5} for this reason our attention will be confined to discussing the role of a temperature dependent electrical conductivity in modifying the electromagnetic force field and the heat generation patterns.

Using the MHD approximation the dimensionless form of the electromagnetic field equation takes the following form:

$$j\alpha\hat{H}^* = -\nabla^* \times \frac{\nabla^* \times \hat{H}^*}{\sigma^*} + Re_m \nabla^* \times (V^* \times \hat{H}^*) \quad [1]$$

where:

$$\hat{H}^* = \hat{H}/H_0, \nabla^* = L_0 \nabla, V^* = V/V_0, \sigma^* = \sigma/\sigma_0 \quad [2]$$

\hat{H} = complex amplitude of the magnetic field intensity,

V = velocity vector,

σ = electrical conductivity,

$H_0, V_0,$

σ_0, L_0 = reference values for \hat{H}, V, σ and the length scale respectively,

$$j = \sqrt{-1},$$

$$\alpha = \omega \sigma_0 \mu_0 L_0^2, \quad [3a]$$

$$Re_m = L_0 V_0 \sigma_0 \mu_0 \text{ is the magnetic Reynolds Number,} \quad [3b]$$

ω = angular frequency of current, and

μ_0 = magnetic permeability of free space.

In contrast, the equivalent expression for the case of constant electrical conductivity is:

$$j\alpha\hat{H}^* = \nabla^{*2}\hat{H}^* + Re_m \nabla^* \times (V^* \times \hat{H}^*) \quad [4]$$

For a small scale system (electrode radius = 0.03 m, mold radius = 0.05 m, current = 1.7 kA, $\sigma_0 = 250 \text{ mho} \cdot \text{m}^{-1}$, $\omega = 377 \text{ radians/s}$) considered in an earlier paper,⁵

$$\alpha \approx 1.2 \times 10^{-3}, Re_m \approx 1.6 \times 10^{-6}$$

For a large scale system to be considered in this paper (electrode radius = 0.22 m, mold radius = 0.33 m, current = 18 kA $\sigma_0 = 218.5 \text{ mho} \cdot \text{m}^{-1}$, $\omega = 12.6 \text{ radians/s}$),

$$\alpha \approx 1.5 \times 10^{-3}, Re_m \approx 1.4 \times 10^{-5}$$

It follows that since

$$\alpha, \text{ and } Re_m \ll 1$$

the spatial distribution of H will not be affected by

Table I. Physical Property Values Used

K	thermal conductivity of slag	6.92 W/(m · K)
C_p	specific heat of slag	1255 J/(kg · K)
ρ	density of slag	2.8×10^3 kg/m ³
β	coefficient of expansion of slag	1×10^{-4} K ⁻¹
μ	viscosity of slag	2.5×10^{-2} kg/(m · s)
σ	electrical conductivity of slag	(ohm · m) ⁻¹
	$\ln \sigma = -6769.0/T + 8.818$	

Table II. Numerical Values of the Parameters used in the Computation

R_e	electrode radius	0.22 m
R_m	mold radius	0.33 m
L	slag depth	0.23 m
ω	angular frequency of current	12.6 radians/s
\bar{I}_0	current	18.0 kA
μ_0	magnetic permeability of free space	1.26×10^{-6} Henry/m

either the frequency effect associated with AC operation or by the fluid motion. Let us rearrange Eq. [1] to obtain:

$$j\alpha\sigma^*\hat{H}^* = \nabla^2\hat{H}^* + \nabla^*\ln\sigma \times \hat{J}^* + \sigma^*Re_m\nabla^*\times(V^*\times\hat{H}^*) \quad [5]$$

where \hat{J} denotes the amplitude of the current density vector. For the very small magnetic Reynolds numbers encountered it is the second term on the r.h.s. of Eq. [5] that represents the influence of the temperature field (through the variation of the electrical conductivity) on the magnetic field.

On noting that the temperature dependence of the electrical conductivity is often expressed as:

$$\sigma = Ae^{-B/T} \quad [6]$$

one can write

$$\ln\sigma^* = \gamma \left[1 - \frac{1}{T^*} \right] \quad [7]$$

where

$$T^* = T/T_0; \quad \gamma = B/T_0 \quad [8]$$

and T_0 is a suitable average temperature of the slag. Using Eq. [7], the second term on the r.h.s. of Eq. [5] can be expressed as:

$$\nabla^* \ln\sigma^* \times \hat{J}^* = \frac{\gamma}{T^*} \nabla^* \ln T^* \times \hat{J}^* \quad [9]$$

For cylindrical coordinates with axial symmetry, Eq. [9] takes the following form:

$$\nabla^* \ln\sigma^* \times \hat{J}^* = \frac{\gamma}{T^*} \left[\hat{j}_r^* \frac{\partial \ln T^*}{\partial z^*} - \hat{j}_z^* \frac{\partial \ln T^*}{\partial r^*} \right] \quad [10]$$

since $J_z^* \gg J_r^*$ over most of the domain, the principal influence of the temperature dependence of the electrical conductivity is associated with the

$\left[-\frac{\gamma}{T^*} \hat{j}_z^* \frac{\partial \ln T^*}{\partial r^*} \right]$ term which tends to be positive over most of the domain. It follows, on reexamining Eqs. [4] and [5], that the magnetic field will tend to be higher when the temperature dependence of the

electrical conductivity is taken into account.

In the following we shall illustrate these effects by working a concrete example, representing the behavior of a typical, large scale ESR system, the property values of which are given in Table I. The parameters used in the computation are listed in Table II.⁷ The numerical technique employed in performing the calculations has been described in Ref. 6.

In Figs. 1 through 4 we shall present a selection of the computed results. In all these graphs the curves drawn with the solid lines have been computed, by neglecting the effect of the velocity field on H and by taking constant value for the electrical conductivity.

The curves drawn by the broken lines represent:

i) calculations in which an allowance is made for the temperature dependence of the electrical conductivity of the slag and for the convection of H .

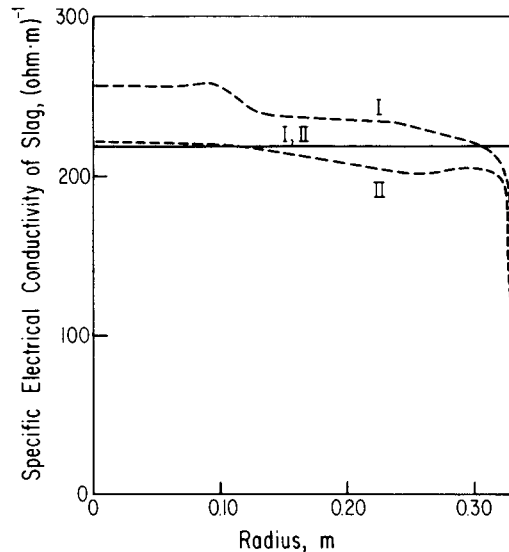


Fig. 1—Radial distribution of the electrical conductivity of the slag. — calculation using a uniform value (218.5 Ohm⁻¹ · m⁻¹) for the electrical conductivity; — — calculation using a temperature dependent electrical conductivity, calculated power input in both cases 1.24 MW. I: 0.041 m below the electrode—slag interface; II: 0.167 m below the electrode—slag interface.

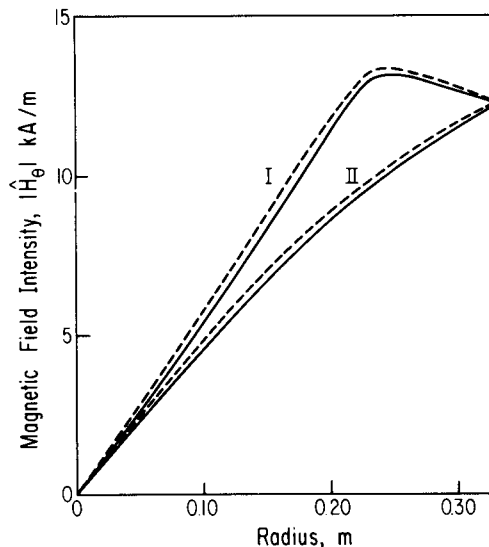


Fig. 2—Radial distribution of the magnetic field intensity. Legends same as in Fig. 1.

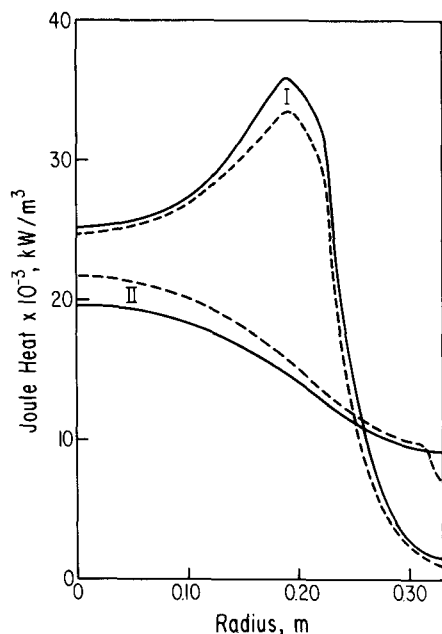


Fig. 3—Radial distribution of the heat generation rate in the slag. Legends same as in Fig. 1.

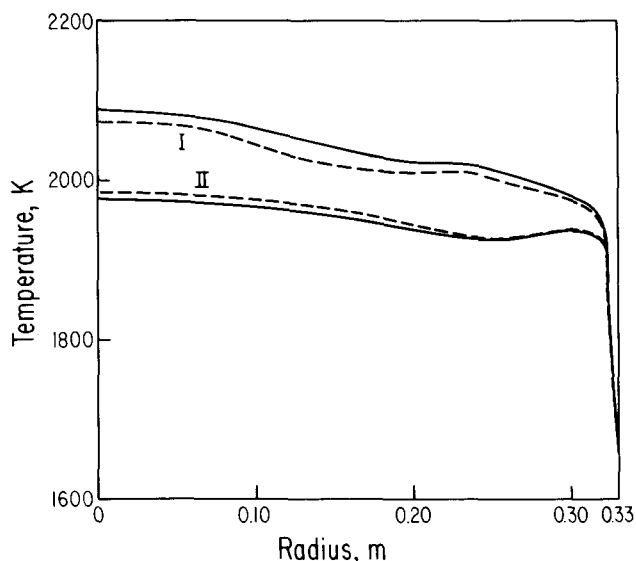


Fig. 4—Radial distribution of temperature in the slag. Legends same as in Fig. 1.

ii) calculations in which an allowance is made for the temperature dependence of the electrical conductivity of the slag but the convective transport of H is neglected.

As expected, convection did not have any effect on the distribution of the magnetic field and calculations i) and ii) gave identical results.

The symbols I and II represent results at two different axial positions—0.041 m and 0.167 m below the slag—electrode interface. Fig. 1 shows the radial distribution of the electrical conductivity of the slag, where it is seen that significant spatial variations have

occurred, especially in the regions close to the mold wall. The solid line represents the uniform value 218.5 ($\text{ohm} \cdot \text{m}$)⁻¹ which gave the same electrical power input (1.24 MW) as the temperature dependent conductivity.

Fig. 2 shows the radial distribution of the magnetic field intensity. It is seen, that as predicted by the asymptotic analysis, the magnetic field intensity, computed for the temperature dependent electrical conductivity tends to be somewhat higher than the values calculated for a constant value of the conductivity.

Fig. 3 shows the radial distribution of the “Joule Heating” in the system, again at two different axial positions.

It is seen that in the vicinity of the electrode (curve I), the “Joule Heating” appears to be more pronounced for the case computed for the temperature independent electrical conductivity, while the reverse is true for curve II depicting the behavior of the system in the vicinity of the slag—metal interface.

The difference in “Joule Heat” distribution at the two axial positions represents the difference in the relative magnitudes of the current and the electrical conductivity at these two locations.

Finally Fig. 4 shows a comparison between the temperature distribution, calculated for constant electrical conductivity and for a temperature dependent electrical conductivity. Paralleling the behavior seen in Fig. 3, close to the electrode the constant electrical conductivity will tend to give higher local temperatures, the maximum difference between the two cases being about 25 K. The behavior found here is rather less extreme than the previously reported difference between constant and variable electrical conductivities. The earlier work⁵ considered a small, laboratory scale system and a slag with a more marked dependence of the electrical conductivity on temperature.

The following conclusions may be drawn from these calculations:

1) For most of the conditions, normally encountered in ESR systems the frequency effect, introduced by the AC conditions do not play a very important role in affecting the electromagnetic force field in the slag phase.

2) For ESR systems the magnetic Reynolds number is small, so that convection in the melt does not affect the current transfer, or the electromagnetic force field.

3) The use of an average electrical conductivity may be acceptable in the modelling of most systems, although the proper allowance for a variable electrical conductivity could have a significant, if not overwhelming effect in the modelling of small, laboratory scale systems where much larger temperature gradients may exist.

The authors wish to thank the National Science Foundation for partial support of this investigation under grant DMR 79-24267.

1. A. H. Dilawari and J. Szekely: *Metall. Trans. B*, 1977, vol. 8B, pp. 227–36.

2. A. H. Dilawari and J. Szekely: *Metall. Trans. B*, 1978, vol. 9B, pp. 77–87.
3. A. H. Dilawari, J. Szekely and T. W. Eagar: *Metall. Trans. B*, 1978, vol. 9B, pp. 371–81.
4. J. Kreyenberg and K. Schwerdtfeger: *Arch. Eisenhüttenwes*, 1979, no. 1, pp. 1–6.
5. M. Choudhary and J. Szekely: *Metall. Trans. B*, 1980, vol. 11B, pp. 439–53.
6. M. Choudhary: A Study of Heat Transfer and Fluid Flow in the Electroslag Refining Process, Sc.D. Thesis, Massachusetts Institute of Technology, Cambridge, Massachusetts, 1980.
7. M. Choudhary and J. Szekely: *Ironmaking and Steelmaking*, 1981, in press.